Can directional resonances be used to map intensely deformed fault zones of Mt. Etna volcano ?

F. Cara[1], G. Di Giulio[1], S. Giammanco[1], G. Lombardo[2], G. Milana[1], M. Neri[1], R. Rigano[2], A. Rovelli[1], N. Voltattorni[1]

1) Istituto Nazionale di Geofisica e Vulcanologia, Italy
2) Università di Catania, Italy

Contacting author digiulio@ingv.it

Seismological Society of America
SSA 2009 Annual Meeting Poster #80

The experiment on Mt. Etna volcano

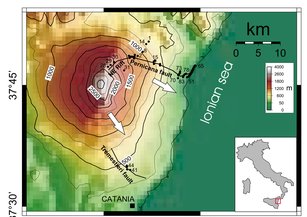

Topographic map of Mt. Etna with the simplified traces of *Pernicana* fault system (*PFS*) and *Tremestieri* fault. The black dots show the **microtremor measurements** performed along the main faults of volcano (data collected from 2006 to 2008).
The white arrows indicate the direction of movement of the unstable south-eastern flank of Mt. Etna.

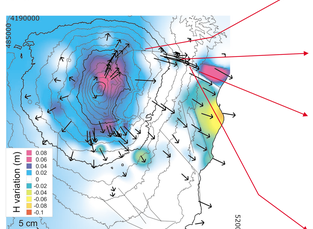

Displacement vectors and height variations from the comparison between July 2005 and June 2006. The arrows represent the horizontal displacement vectors, while the vertical displacement is shown by a colour map obtained by interpolating the measurements relevant to each benchmark (redrawn from *Bonforte et al.*, 2008).

Effects of flank dynamics on walls and roads along the *Pernicana* fault system (*PFS*).

Pictures showing some sites of **seismic noise recordings** along the *Pernicana* fault system. We used Lennartz Le3D-5s sensors with Reftek R130 digitizers.

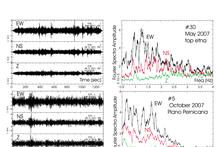

Noise recordings and **Fourier amplitude spectra** of the three components of ground motion. Measurement #30 is close to the crater area; measurement #5 is at *Piano Pernicana*. The spectra of EW, NS and Z components are plotted in black, red and green lines, respectively.

Introduction

Mt. Etna is characterized by flank instability of the eastern to south-western portions of the volcanic edifice, producing down-slope movements with rates up to several decimeters in a month during eruptive events of the 2002-2003 activity. The unstable sector is bounded to the North by a E-W transtensive fault (the *Pernicana* fault system), extending from the *NE Rift* to the coastline of the Ionian Sea for a length of > 18 km. The western portion of the *Pernicana* fault system (close to *Piano Pernicana* area) is characterized by the most intense deformation (*Acocella and Neri*, 2005).
In this area we have performed volcanic tremor measurements on a dense grid along and across the fault zone. Ambient vibration measurements are also performed along a second fault (*Tremestieri* fault) which confines the slip of the eastern flank to the south-east.
The analysis using both microtremors and local earthquakes recorded in these faults shows persistent polarization of ground motion. Horizontal-to-vertical spectral ratios (HVSR) show large directional resonances of horizontal components within the damaged fault zones.
The resonance occurs around 1Hz at *Piano Pernicana*, and around 4 Hz in the *Tremestieri* fault zone.
The resonance amplitude in the HVSRs seems to be fairly well correlated to soil gas anomalous concentrations (in particular, radon and CO2 both considered tracer gases of major crustal discontinuity) in the fault zones, suggesting that both the effects are linked to local fracturing conditions.
According to previous results on velocity anisotropy in the shallow crust, we believe that a role on polarization could be played by stress-induced anisotropy and micro-fracture orientation in the near-surface lavas.
The occurrence of directional resonances, if confirmed in other faults, can be a powerful tool to map buried damaged fault zones on the Mt. Etna volcano.

Microtremor recordings and array experiment at *Piano Pernicana*

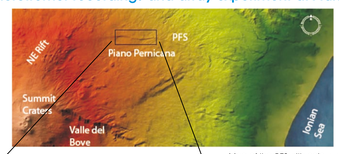

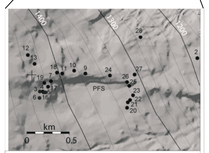

Map of the *PFS* with colour proportional to topography (from blue to red).
The black rectangle indicates the **intensely deformed zone of the *PFS (Piano Pernicana)***, where we concentrated the tremor measurements.

Tremor measurement sites (black circles) at *Piano Pernicana*.
The cross symbol indicate the area where we performed an **array experiment** using both linear geophones with mini-gun source as well as a 2D array of 16 seismological seismometers recording volcanic tremor.

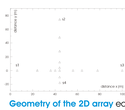

Geometry of the 2D array equipped with long-period seismometers (LE3D/5 s).

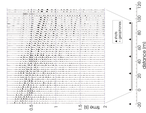

In addition to the 2D array that recorded volcanic tremor, we also deployed in the same area two **small-aperture linear arrays of geophones** using active source. The figure shows an example of **shot recordings** using forty eight 4.5-Hz vertical geophones (unfilled triangles) with regular spacing of 2 m. The black triangles over the linear array indicate the shots positions using a mini-bang source.

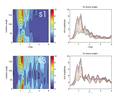

HVSR -as a **function of frequency and direction** of motion- computed on volcanic tremor at four selected stations (s1,s2,s3, and s4) of the 2D array.

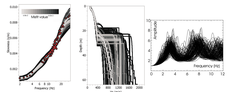

Left) **Dispersion curves** after **inversion** overlaid by the observed phase-velocity (circles) for the vertical component. The dispersion curve in the 2-5 and 7-35 Hz frequency bands was computed using the 2D array of seismological sensors and the two linear arrays of geophones, respectively. Gray tonality is proportional to the misfit computed in the inversion. **Back-azimuth** of about 220° was inferred through *f-k* analysis of tremor data recorded at the 2D array. This value points at the summit crater area.
Middle) 1-D layered **Vs profiles** obtained by inversion.
Right) theoretical **1D transfer functions** (SH case) computed for all models in the middle panel.

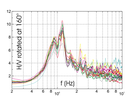

HVSRs, for the 160° rotated motions, of the 16 stations of the 2D array.

Tremor data analysis at *Piano Pernicana*

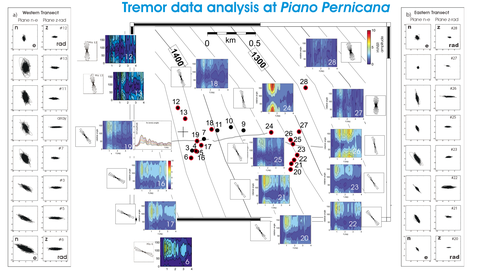

HVSR and **polarization** around the array area (which is indicated by a cross whereas the grey line shows the trace position of the *Pernicana* fault). HVSRs are plotted up to 4 Hz and the maximum value of amplitude scale is 10.
The rose diagrams indicate the results from covariance matrix polarization analysis. Note the **variation of polarization crossing the main trace of the *PFS***; for example measurements sites #6, #17, and #16 show a polarization of about 120° (clockwise from north), measurements #19 and #18 show a polarization of about 160°.
We also show the **particle motion** along two transects crossing the fault. Five minutes of volcanic tremor are band-pass filtered between 0.5 and 2 Hz where we observe the largest **directional effect**. For each transect, the panel on the left hand shows the particle motion in the horizontal plane (n-e). After the rotation to the direction of maximum polarization, the particle motion is plotted in the vertical plane (panel on the right hand, z-rad).

Tremor data analysis along the entire *PFS* and at the *Tremestieri* fault

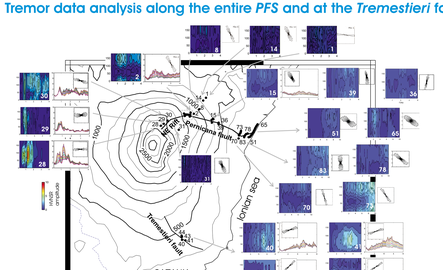

HVSR and **polarization** results of measurements far from the array area (indicated by the dashed rectangle). The gray lines indicate the *NE Rift*, the *PFS* and the *Tremestieri* fault. Measurements #28, #29 and #30 were performed near the *NE Rift*. Measurements from #40 to #44 were conducted near the ***Tremestieri* fault**.

Earthquake data analysis at *Piano Pernicana*

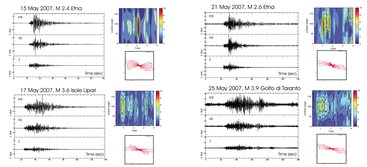

HVSR and polarization analysis on earthquake data at site #5 (*Piano Pernicana* within the *PFS*). The rose diagrams indicate the results of the covariance matrix polarization analysis. We observe consistency of the directional effect using different earthquakes i) between rose diagrams and azimuthal pattern of H/V spectral ratios, and, ii) between earthquake and tremor data analysis.

Earthquake data analysis at the *Tremestieri* fault

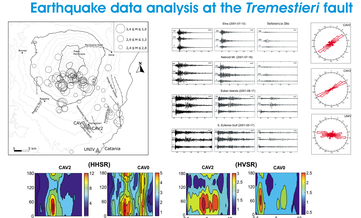

HVSR, HHSR and polarization analysis on earthquake data at the *Tremestieri* fault (*Rigano et al.*, 2008). Sites CAV2 and CAV0 were installed in area of the *Tremestieri* fault whereas UNIV was a reference site. Earthquake results show frequency and direction of polarization in good agreement with noise results.

Soil-gas radon concentration

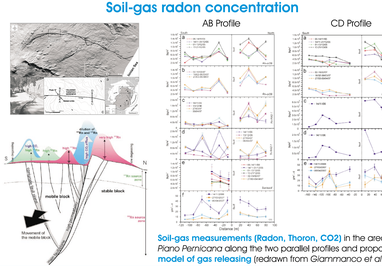

Soil-gas measurements (Radon, Thoron, CO2) in the area of *Piano Pernicana* along the two parallel profiles and proposed **model of gas releasing** (redrawn from *Giammanco et al.*, 2009).

Conclusions

The main purpose of this study was to check if seismic noise horizontal polarization can be associated to the main faults on Mt. Etna volcano.
HVSR and polarization of volcanic tremor data highlighted that:

1) strong directional resonances characterize the horizontal components of ground motion in the intensely deformed fault zones of the *Pernicana* fault system (*Piano Pernicana*) as well as in the *Tremestieri* fault.
2) earthquake records yield the same result, suggesting a local role of the fault properties in generating directional effects.

Although the actual cause of polarization is unknown, a role of stress-induced anisotropy and micro-fracture orientation in the near-surface lavas of the fault zones can be hypothesized consistently with the sharp rotation of the polarization angle observed in the intensely deformed area.

Acknowledgments. A part of this research was conducted with internal research funds of Department of Seismology and Tectonophysics of INGV-Rome.
A significant contribution by Project *V4-Flank* of the *DPC-INGV* agreement of 2008-2010 is also acknowledged.

References

Acocella, V. and M. Neri (2005). Structural features of an active strike-slip fault on the sliding flank of Mt. Etna (Italy), *J. Struct. Geol.*, 27(2), 343-355.
Bonforte, A., A. Bonaccorso, F. Guglielmino, M. Palano, and G. Puglisi (2008), Feeding system and magma storage beneath Mt. Etna as revealed by recent inflation/deflation cycles, *J. Geophys. Res.*, 113, B05406, doi:10.1029/2007JB005334.
Rigano, R., F. Cara, G. Lombardo, and A. Rovelli (2008), Evidence for ground motion polarization on fault zones of Mt. Etna volcano, *J. Geophys. Res.*, 113, B10306, doi:10.1029/2007JB005574.
Giammanco, S., G. Immè , G. Mangano, D. Morelli and M. Neri (2009), Comparison between different methodologies for detecting radon in soil along an active fault: The case of the Pernicana fault system, Mt. Etna (Italy), *Appl. Radiat. Isot.*, 67, 178-185.